Pharmacogn. Mag.
A multifaceted peer reviewed journal in the field of Pharmacognosy and Natural Products
www.phcog.com | www.phcog.net

ORIGINAL ARTICLE

Preparation of a Nanoemulsified Drug Delivery System of Astilbin using Edible Formulation Components: *In vivo* Evaluation of Oxaliplatin-Induced Cirrhotic Liver Injury

Yixing Wang, Xuping Zhang[1], Jin Zhou[2], Shilei Xu, Xiaodan Kou, Yuan Cheng[3]

Department of Pharmacy, Sichuan Cancer Hospital and Institute, Sichuan Cancer Center, Medicine School of University of Electronic Science and Technology, [1]Department of Pharmacy, Chengdu Second People's Hospital, [2]Department of Oncology, Sichuan Cancer Hospital and Institute, Sichuan Cancer Center, Medicine School of University of Electronic Science and Technology, [3]Department of pharmacology laboratory, Hospital of Chengdu University of Traditional Chinese Medicine, Chengdu, Sichuan, China

Submitted: 24-Jul-2021 Revised: 04-Dec-2021 Accepted: 25-Jan-2022 Published: 07-Jul-2022

ABSTRACT

Background: Astilbin is a flavonoid phytoconstituent extracted from Chinese herb Rhizoma Smilacis Glabrae, a common Chinese food ingredient. **Objectives:** The present study used astilbin as a model drug to develop food-based nanoemulsified formulations. These formulations were then tested for their possible role in countering Oxaliplatin (OXP) associated oxidative stress. **Materials and Methods:** Thirty six healthy male BALB/c mice of age 10–12 weeks and weight 25–30 g were included in the present study. The mice were administered OXP through intraperitoneal route in a dose of 8 mg/kg for a period of 4 days. The animals in the control group were administered a 10 ml/kg dose of 5% (w/v) glucose solution. For evaluating the hepatoprotective effect of developed formulations on OXP-induced liver injury, the animals from treatment groups were administered once daily dose of drug loaded formulations 60 min before OXP treatments (200 mg/kg equivalent of formulation, intraperitoneally) for 4 days. Finally, the blood and hepatic tissue samples were obtained for future analysis. **Results:** We successfully developed non-toxic nanoemulsion systems for astilbin, which comprised of different non-toxic food ingredients of astilbin and evaluated the potential reversing the OXP induced liver injury. The food-based nanoemulsions possessed attractive physical properties and exhibited sufficient stability profile when subjected to freeze-thaw cycles as well as 6-month storage at ambient and cold temperatures. Furthermore, excellent cumulative *in vitro* drug permeation was reported for the prepared formulations through dialysis membrane bags. We also observed the significant reduction in biomarkers of hepatic oxidative stress, caused by OXP chemotherapy in experimental mice, thereby indicating a marked reversal of liver injury. **Conclusion:** We concluded that nanoemulsified astilbin can be used as therapeutic agent to counter OXP-associated oxidative stress.

Key words: Astilbin, cirrhosis, liver injury, nanoemulsion, oxaliplatin

SUMMARY

- Astilbin is a flavonoid phytoconstituent extracted from Chinese herb Rhizoma Smilacis Glabrae, a common Chinese food ingredient. The present study used astilbin as a model drug to develop food-based nanoemulsified formulations. These formulations were then tested for their possible role in countering Oxaliplatin (OXP)-associated oxidative stress. The mice were administered OXP through intraperitoneal route. For evaluating the hepatoprotective effect of developed formulations on OXP-induced liver injury, the animals from treatment groups were administered once daily dose of drug loaded formulations before OXP treatments. Finally, the blood and hepatic tissue samples were obtained for future analysis. The food-based nanoemulsions possessed attractive physical properties and exhibited sufficient stability profile when subjected to freeze-thaw cycles as well as 6-month storage at ambient and cold temperatures. Furthermore, excellent cumulative *in vitro* drug permeation was reported for the prepared formulations through dialysis membrane bags. We also observed the significant reduction in biomarkers of hepatic oxidative stress, caused by OXP chemotherapy in experimental mice, thereby indicating a marked reversal of liver injury. We concluded that nanoemulsified astilbin can be used as therapeutic agent to counter OXP-associated oxidative stress.

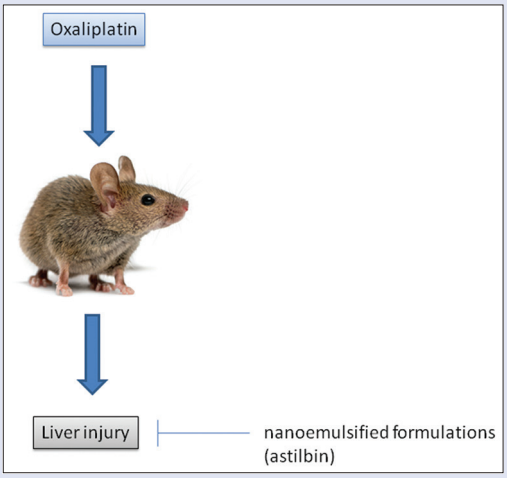

Abbreviations used: OXP: Oxaliplatin; IL: Interleukin; SOD: Superoxide dismutase; GSH: Glutathione peroxidase; MDA: Malondialdehyde; TEM: Transmission electron microscopy; PTA: Phosphotungstic acid; RIPA: Radioimmunoprecipitation assay; BCA: Bicinchoninicz.

Correspondence:

Dr. Yuan Cheng,
Pharmacology Laboratory, Hospital of Chengdu University of Traditional Chinese Medicine, No. 39 Shi-er-qiao Road, Chengdu, Sichuan 610072, China.
E-mail: yuancheng372@gmail.com
DOI: 10.4103/pm.pm_345_21

Access this article online
Website: www.phcog.com
Quick Response Code:

Cite this article as: Wang Y, Zhang X, Zhou J, Xu S, Kou X, Cheng Y. Preparation of a nanoemulsified drug delivery system of astilbin using edible formulation components: *In vivo* evaluation of oxaliplatin-induced cirrhotic liver injury. Phcog Mag 2022;18:321-7.

INTRODUCTION

Oxaliplatin (OXP) is a third-generation platinum-based anticancer drug and is commercialized worldwide under the trade name Eloxatin. OXP-based chemotherapies are extensively utilized for the treatment for solid organ malignancies, particularly colorectal cancers.[1] Although it is known for its beneficial effects, it has also been associated with severe toxicities, specifically, neurotoxicity, white-blood cell disorders and liver toxicity.[2,3] Particularly, it has been reported that, OXP-based treatment cycles result in severe hepatotoxicity and varying degrees of liver injury.[4-6] At present, there is no approved treatment or regimen for addressing the OXP-induced hepatotoxicity. Moreover, as the patients receiving chemotherapy are already administering variety of drugs, adding another treatment and treatment regimen will generally cause increased medication burden and may result in low patient compliance and adherence. It could be therefore a logical approach to design a therapeutic regimen comprising of non-toxic, biofriendly and more preferably food-based ingredients. To the best of our knowledge, we are the first research team to attempt the development of a nanoemulsified drug delivery system consisting entirely phytoingredients and food materials for addressing the issue of acute liver injury occurring after OXP chemotherapy.

Astilbin is a flavonoid phytoconstituent extracted from Chinese herb Rhizoma Smilacis Glabrae, a common Chinese food ingredient [Figure 1]. It is known to have potential therapeutic effects, such as immunosuppressant activity due to T-cell anti-proliferation, antioxidant efficacy owing to it free-radical scavenging ability and hypersensitivity reaction inhibition due to modulator effects on cytokine Interleukin (IL)-10.[7-10] Owing to these properties, astilbin has been hailed as an excellent hepatoprotective agent for use in variety of hepatotoxic conditions. Therefore, we used astilbin as a model drug in our development of food-based nanoemulsified formulations. The formulation was prepared using several food ingredients such as edible oils, edible oil-based surfactants, and purified water. We successfully prepared and preliminarily evaluated non-toxic food-based nanotherapeutic medication. The developed systems possessed desirable physical properties, particularly uniformly distributed nanosized globules, excellent drug loading capacity and performed satisfactorily to permeate drug in simulated gastric and intestinal fluids. Further, our preliminary *in vivo* studies indicated significant reversal of oxidative stress in OXP-treated lab mice indicated the therapeutic potential of these nanoemulsified formulations.

MATERIALS AND METHODS

Materials

The drugs and speciality kits used in our studies, i.e., astilbin, OXP, superoxide dismutase (SOD) kit, glutathione peroxidase (GSH) kit, malondialdehyde (MDA) kit and total protein quantification kit (Bicinchoninicz method) were purchased from Sigma Aldrich Co., USA. Food grade fixed oils like coconut oil (purity: 98.7%, density: 0.903 g/mL at 25°C) castor oil, (purity: 98%, density: 0.961 g/mL at 25°C) soybean oil (purity: 99.2%, density: 0.90 g/mL at 25°C) canola oil (purity: 99.6%, density: 0.913 g/mL at 25°C), palm oil (purity: 99.5%, density: 0.89 g/mL at 25°C), cottonseed oil (purity: 99.2%, density: 0.89 g/mL at 25°C), peanut oil (purity: 99.8%, density: 0.91 g/mL at 25°C) and sunflower oil (purity: 99.2%, density: 0.91 g/mL at 25°C), and aromatic oils like lemon oil (purity: 99.7%, density: 0.82 g/mL at 25°C), orange oil (purity: 99.8%, density: 0.81 g/mL at 25°C), eucalyptol oil, (purity: 73.7%, 0.89 g/mL at 25°C) and clove oil (purity: 99.1%, density: 1.01 g/mL at 25°C) were procured from local pharmacy. Plant derived surfactants including linoleoyl polyoxylglyceride (LPO) (Acconon CMG-6), lauroyl macrogoglycerides (Acconon C-44), polyoxyethylene-20 sorbitol (P2S) (Acconon Sorb-20), ethoxylated oleic acid (EOA) (Acconon 400 MO) and polyoxypropylene-11 stearyl ether (Acconon E) were purchased from Abitec Corp. USA. All other chemicals and reagents used were purchased from local market and were of analytical grade.

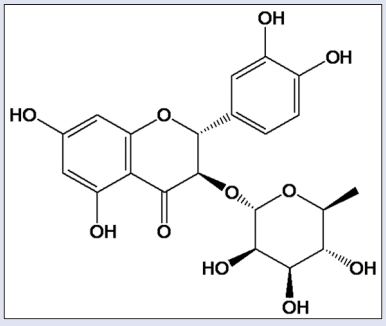

Figure 1: Chemical structure of astilbin

Solubility study

The saturation solubility of astilbin was determined in various edible oils using previously established shaking flask method. Briefly, excess amount of the drug was added in oils placed in glass vials. The vials were shaken for 48 h in a solubility orbital shaker apparatus (E20/80, Orbital Shaker-Incubator|, Biosan Ltd. USA) at a temperature of 37°C. Thereafter, the supernatants were filtered and analyzed by Ultraviolet spectroscopy (UH4150, Hitachi Corp., Japan).

Pseudoternary phase diagram construction

Pseudoternary phase diagrams were constructed to screen nanoemulsion components, which provide largest monophasic regions. The surfactant and co-surfactant were weighed in each screw-capped glass vials to produce various ratios (1:0.1, 1:0.25, and 1:0.5, w/w) and were shaken vigorously for 30 s to afford the required surfactant mixtures. Thereafter, the oils and the prepared surfactant mixtures were placed in test tubes to provide various ranging from 9.5:0.5 to 0.5:9.5 (w/w). Distilled water was added in small aliquots to each oil-surfactant mixture with gentle vortex mixing to allow equilibration, and visually examining physical behaviour of obtained system each time. The fluid transparent mixtures were defined as the nanoemulsions and the fluid translucent regions were defined as emulsions. Finally, the nonflowing semisolid regions were termed as emulgels.

Preparation of drug loaded nanoemulsions

The drug loaded nanoemulsions were prepared using simple vortex mixing. The selected oils and surfactant combinations in weighed quantities were placed in a glass vial and were stirred until clear mixtures were obtained, and thereafter astilbin was solubilized in these mixtures. It involves mixing of selected oil of 18.5% with surfactant 81.5%. Afterward, distilled water was added drop wise with continuous shaking to obtain transparent drug loaded nanoemulsions.

Characterization of nanoemulsions

The globule size, surface charge (zeta potential), polydispersity index and electrical conductivity of the nanoemulsions were determined using a dynamic light scattering based particle size analyzer (Zetasizer Nano-ZS; Malvern Co., UK) equipped with a 4 mW He-Ne laser at scattering angle of 173°C.

Transmission electron microscopy (TEM) was used to determine the morphology of nanoemulsion globules (T-7000, Hitachi Ltd., Japan).

One drop of diluted nanoemulsion samples was negatively stained by 2% phosphotungstic acid (PTA) solution and placed on film-coated copper grids, and the excess sample was removed with filter paper. After drying, the sample was visualized under the TEM.

The rheological behavior of prepared nanoemulsions was evaluated with rheometer (Paar Physica MC1, Brookfield DV-II, UK), equipped with peltier cylinder cartridge (cup and bob). The analysis was performed at a temperature of 25°C, with a shear rate ranging from 1 to 97 s^{-1}.

Physical stability study

The nanoemulsions were placed in sealed in glass vials and vertically stored for 16 h in a freezer at −21°C and then for 8 h at room temperature (25°C ± 2°C). The nanoemulsions were observed for any physical change. This cycle was repeated three times.[11] The nanoemulsions were also subjected to a 6-month stability evaluation study. The nanoemulsion samples placed in screw capped glass vials were kept at 4°C and 30°C, and after 6 months the nanoemulsions were observed for any physical changes such as color, consistency, globule sizes, and drug content.

In vitro permeation study

The *in vitro* release study of prepared formulations was evaluated using a dialysis bag method reported previously with slight modifications.[12] Briefly, tubular dialysis membrane (10K MWCO, Hi-Media Industries Inc., USA) pieces were soaked in ionized water for 12 h prior to conducting the release studies. Thereafter, 10 mL of drug loaded and control formulations were placed in dialysis tube bags prepared from the dialysis tubes by sealing the tube portions firmly at both ends. Two types of release media, namely 0.1 N HCl and phosphate buffer saline (pH 6.5) were used in the *in vitro* release studies to simulate the gastric and intestinal fluids, respectively. There formulation filled bags were immersed in flasks containing 300 mL of the release media maintained 37°C, which was stirred at 100 rpm using magnetic stirrer beads. At predetermined intervals (5, 15, 30, 45, 60 and 90 min), aliquots of 2 mL of release medium were withdrawn and replaced immediately with equal volumes of fresh release medium. For comparative propose, the drug was solubilized in coconut oil to prepare oil solution, which was subjected to the *in vitro* release study similarly to the drug-loaded nanoemulsion formulations (hereinafter, operational data store [ODS]). The samples were filtered through 0.22 µm filter membranes, and the analysis of drug released was performed using high-performance liquid chromatography system (A-1200 series, Agilent Inc., USA) which consisted of a quart pump, a degasser, a Rheodyne 7125 injector with a 20 µL loop.

In vivo hepatic oxidative stress model

All animal studies were performed as per the protocols approved by of the Animal Ethical Committee of University of Traditional Chinese Medicine (Sichuan, China) (No: C53736/19). The institutional guidelines were strictly followed while performing the animal studies.

Thirty six healthy male BALB/c mice of age 10–12 weeks and weight 25–30 g were procured from Institute Animal Breeding Center (XYS, India). The animals were kept at a temperature of 25°C ± 2°C in polypropylene animal cages and were allowed to acclimatize for a period of 1 week with 12 h day-and-night cycle (white light on between 8.00 a.m. and 8.00 p.m.). The animals were fed standard rodent diet (Envigo Diets, UK Ltd.) and drinking water was provided *ad libitum*.

The mice were administered OXP via intraperitoneal route in a dose of 8 mg/kg for a period of 4 days based on previous reports.[13-15] The animals in control group were administered a 10 ml/kg dose of 5% (w/v) glucose solution. There were six mice in each treatment group. After 12 h of OXP injection until the end of the experiment, mice were randomly sacrificed with cervical dislocation. Separately, animals were provided anesthetize using isoflurane (2%), and an abdominal incision was made, before withdrawing blood and hepatic tissue samples. The blood samples were collected from the experimental animals after 6 weeks of treatment from the retro-orbital vein. For evaluating the hepatoprotective effect of developed formulations on OXP-induced liver injury, the animals from treatment groups were administered once daily dose of drug loaded formulations 60 min prior to OXP treatments (200 mg/kg equivalent of formulation, intraperitoneally) for 4 days. The animals were euthanized by cervical dislocation after the final chemotherapy dose. Finally, the blood and hepatic tissue samples were obtained for future analysis.

Serum alanine aminotransferase and aspartate aminotransferase level estimation

Blood samples obtained from animals were centrifuged (Beckman Coulter Inc., USA) for 10 min at 300 ×g, and the isolated supernatants were analyzed using alanine aminotransferase and aspartate aminotransferase kits (Sigma Aldrich Inc., USA), as per the protocol provided by manufacturer. The results are represented as units/l.

Oxidative stress biomarkers

Liver tissues proteins were isolated in Radio immune precipitation assay buffer and quantification was performed using Bradford assay (Sigma Aldrich Inc., USA). The quantification of various oxidative stress biomarkers such as GSH, MDA and SOD was performed using the respective kits (Sigma Aldrich Inc., USA) as per instructions provided by manufacturer.

Statistical analysis

All results represent mean ± standard deviation from experiments preformed in triplicate or hexaplicate parallel runs. Statistical comparison was performed using One-way analysis of variance with Tukey's test. Differences of $P < 0.05$ were considered statistically significant. Analysis was performed using GraphPad InStat™ software (GraphPad Software Inc., USA).

RESULTS AND DISCUSSION

The first step of the study was to analyse the drug solubility in different nanoemulsion components. For our investigations, plant-derived oils, surfactants and co-surfactants were used because the ideal nanoemulsion components should have minimal or no toxicity in addition to high degree of drug solubility. The solubility of astilbin has been presented in Table 1. Among the oils, coconut oil, castor oil and palm oil showed highest drug solubilization ability. Also among the surfactants, P2S, EOA and LPO exhibited greatest drug solubility in respective order. Benzyl alcohol (BA) was the co-surfactant, which showed maximum astilbin carrying capacity.

Thereafter, the step of selecting suitable surfactant co-surfactant for further studies was performed. An ideal surfactant and co-surfactant mixture should not only aid the drug solubilization tendency of oil core of nanoemulsion, but also reduce the interfacial tension to a maximum extent. As mentioned earlier, three surfactants, namely P2S, EOA and LPO provided best astilbin solubility. Also, BA was preferred co-surfactant as it in addition to providing excellent drug solubility, is also least volatile among the studies co-surfactants. The least amount of a surfactant and co-surfactant composite (SC_{min}), which is required to emulsify a mixture of 1 g each of oils and water was studied. The results have been reported in Table 2. It was observed that for all three oils, minimum SC_{min} values were provided by P2S + BA and LPO + BA combinations (1:0.5, w/w). Therefore, for pseudo-ternary phase

behaviour analysis, the two surfactant and co-surfactant compositions were adopted along with the three oils.

The pseudoternary diagrams for the selected oils and surfactant combinations are shown in Figure 2. The phase diagrams constructed with castor oil exhibited large regions of undesirable phases, i.e., emulsion phase and emulgel phase. In contrast, the phase diagrams of coconut oil exhibited very minute regions of emulsion phase. Additionally, noticeably higher nanoemulsion region was located in the phase diagrams prepared with coconut oil. Similar high nanoemulsion region and miniscule emulsion region was observed for palm oil and P2S + BA phase diagram. Therefore, nanoemulsions prepared by coconut oil, P2S + BA, LPO + BA and water; and palm oil, P2S + BA and water are expected to provide most stable nanoemulsion systems, with minimum possibility of phase conversion. Hence, these components were utilized to prepare our drug loaded nanoemulsions.

Table 1: Solubility of astilbin in various solvents at 25°C (mean±standard deviation, *n*=3)

Category	Components	Solubility (mg/mL)
Oils	Coconut oil	4.713±0.341
	Castor oil	3.609±0.101
	Soybean oil	0.677±0.062
	Canola oil	1.733±0.038
	Palm oil	3.230±0.012
	Cottonseed oil	2.002±0.211
	Peanut oil	1.081±0.081
	Sunflower oil	0.544±0.019
Surfactant	Linoleoyl polyoxylglyceride	11.321±1.925
	Ethoxylated oleic acid	14.020±1.032
	Polyoxypropylene-11 stearyl ether	5.980±0.887
	Polyoxyethylene-20 sorbitol	19.544±2.548
	Lauroyl macrogoglycerides	7.719±0.851
Co-surfactants	Lemon oil	7.001±1.144
	Orange oil	3.709±0.731
	Eucalyptol oil	5.603±2.003
	Clove oil	11.092±1.912
	Benzyl alcohol	27.544±2.992

The compositions and characteristics of prepared nanoemulsions have been provided in Table 3. Globule diameter size is considered an imperative parameter as it affects nanoemulsion stability, intestinal permeation and hence ultimately *in vivo* efficacy. The nanosize nature of globules provides greater interfacial area, which ensures larger surface to allow drug release and permeation. The prepared nanoemulsions exhibited mean globule diameters in range of 118 nm to 425 nm, i.e., below the desired value 500 nm for oral absorption.[16] Figure 3a shows the globule size of a representative nanoemulsion. As depicted in Figure 3b, the zeta potential of the nanoemulsion was found to be slightly positive, which indicated that the preparation was sufficiently stable. The positive charge could be attributed to mildly basic nature of astilbin, and it is known that a feeble surface charge can provide great physical stability in nanoemulsified system by preventing aggregation and globules due to electrostatic repulsion owing to the positive zeta potential.[17] Also, the mean polydispersity index values of the nanoemulsions ranged from 0.09 to 0.34, approximately, which is an indicator of sufficient physical stability and shelf life.[18] The morphology of nanoemulsions determined using transmission electron photomicrographs was found to be spherical in shape, which was in agreement with some previous reports [Figure 4].

Finally, the prepared nanoemulsions exhibited desired viscosity at 37°C ranging from 40.22 to 58.07 cps × 10^3. Moreover, the viscosity was not affected significantly ($P > 0.05$) after loading the formulations with astilbin. The viscosity characteristics of nanoemulsions were acceptable from manufacturability point of few.

Table 2: Emulsification tendency of various surfactant and co-surfactant composites at 25°C (mean±standard deviation, *n*=3) for 2 g of oil and water mixtures (1:1, w/w)

Mixture type	Surfactant and co-surfactant combinations	Amount required to emulsify, SC_{min} (g)	Transmittance of obtained emulsions
Coconut oil + water	P2S + BA (1:0.1, w/w)	1.822±0.018	94.2±2.1
	P2S + BA (1:0.25, w/w)	1.219±0.007	95.6±1.7
	P2S + BA (1:0.5, w/w)	0.520±0.222	97.2±2.3
	EOA + BA (1:0.1, w/w)	3.112±0.048	86.2±1.2
	EOA + BA (1:0.25, w/w)	2.633±0.056	87.6±2.3
	EOA + BA (1:0.5, w/w)	1.006±0.009	90.1±1.1
	LPO + BA (1:0.1, w/w)	2.302±0.032	93.2±1.3
	LPO + BA (1:0.25, w/w)	1.890±0.012	94.6±1.0
	LPO + BA (1:0.5, w/w)	1.026±0.066	95.1±1.3
Castor oil + water	P2S + BA (1:0.1, w/w)	2.612±0.099	96.6±1.6
	P2S + BA (1:0.25, w/w)	2.004±0.013	96.9±1.7
	P2S + BA (1:0.5, w/w)	1.446±0.098	97.6±0.9
	EOA + BA (1:0.1, w/w)	5.822±0.337	88.8±2.2
	EOA + BA (1:0.25, w/w)	4.993±0.025	90.2±1.3
	EOA + BA (1:0.5, w/w)	3.636±0.920	93.2±0.6
	LPO + BA (1:0.1, w/w)	3.162±0.076	92.0±1.1
	LPO + BA (1:0.25, w/w)	2.771±0.081	93.7±0.8
	LPO + BA (1:0.5, w/w)	2.567±0.078	94.5±1.5
Palm oil + water	P2S + BA (1:0.1, w/w)	2.432±0.024	95.6±2.1
	P2S + BA (1:0.25, w/w)	1.217±0.031	97.3±0.9
	P2S + BA (1:0.5, w/w)	1.220±0.092	98.1±1.3
	EOA + BA (1:0.1, w/w)	3.652±0.761	82.8±2.3
	EOA + BA (1:0.25, w/w)	3.033±0.121	87.7±0.7
	EOA + BA (1:0.5, w/w)	2.156±0.057	88.1±1.1
	LPO + BA (1:0.1, w/w)	2.671±0.041	93.9±2.3
	LPO + BA (1:0.25, w/w)	2.210±0.046	94.3±1.3
	LPO + BA (1:0.5, w/w)	1.440±0.013	96.8±0.8

BA: Benzyl alcohol; EOA: Ethoxylated oleic acid; LPO: Linoleoyl polyoxylglyceride; SC: Surfactant composite; P2S: Polyoxyethylene-20 sorbitol

Table 3: Compositions and characteristics of selected nanoemulsions

Formulation code	Oil content (%)	Surfactant content (%)	Water content (%)	Globule size (nm)	Polydispersity index	Zeta potential (mV)	Viscosity (cps×10^3)
CPB-1	5	15	80	264.3±7.3	0.318±0.02	7.2±1.8	52.1±3.8
CPB-2	5	20	75	118.2±4.7	0.051±0.07	9.6±1.5	44.62±4.9
CPB-3	10	20	70	404.1±10.2	0.164±0.05	11.4±3.8	58.07±5.1
CLB-1	5	15	80	184.3±2.9	0.029±0.03	7.1±2.7	52.22±6.7
CLB-2	5	20	75	123.2±6.3	0.109±0.04	12.3±3.4	55.33±2.8
CLB-3	10	20	70	425.6±8.2	0.302±0.03	10.0±1.4	50.08±3.9
PPB-1	5	15	80	329.0±5.5	0.253±0.03	8.6±1.5	48.16±3.7
PPB-2	5	20	75	167.6±4.8	0.088±0.02	11.3±1.2	40.22±4.2
PPB-3	10	20	70	301.4±3.9	0.340±0.06	12.4±2.8	47.01±3.3

CPB nanoemulsions-oil phase: Coconut oil, surfactant: P2S + BA; CLB nanoemulsions-oil phase: Coconut oil, surfactant: P2S + BA; PPB nanoemulsions-oil phase: palm oil, surfactant: P2S + BA. The nanoemulsions loaded with 0.5%, 1% and 2% GMH. The globule size, polydispersity index and viscosity of selected nanoemulsion values are expressed as mean±SD (n=3). SD: Standard deviation, BA: Benzyl alcohol; P2S: Polyoxyethylene-20 sorbitol; CPB: Coconut oil, P2S + BA; CLB: Coconut oil, Linoleoyl polyoxylglyceride + BA; PPB: palm oil, P2S + BA

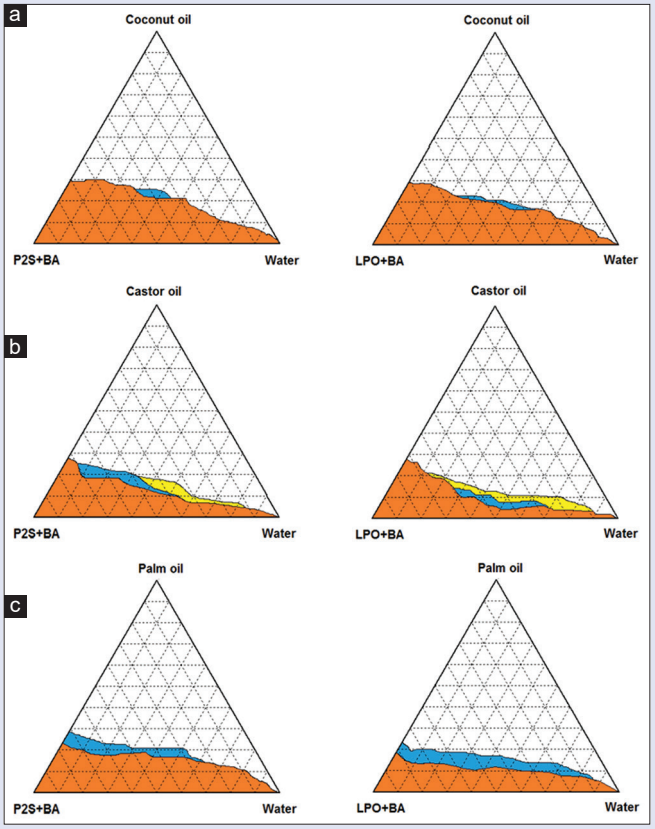

Figure 2: Phase diagrams constructed with edible oils, surfactant mixtures (vegetable based surfactant and Benzyl alcohol, 1:0.5 w/w); The orange shaded area represents o/w nanoemulsion region, the blue and yellow shaded region correspond to opaque emulsion and emulgel regions, respectively. a) nanoemulsions prepared by coconut oil, b) nanoemulsions prepared by caster oil and c) nanoemulsions prepared by palm oil

The freeze thaw cycles showed showed no signs of breaking of nanoemulsion and no drug precipitation. Similarly, the 6-month storage at ambient and cold temperatures exhibited no noticeable differences in the nanoemulsion formulations. Also, no changes in physical characters like colour, transparency or viscosity were observed following both stability protocols. Moreover, there were no significant (P > 0.05) differences observed in IL-nanoemulsion characteristics including mean globule sizes, polydispersity indices and drug load assays.

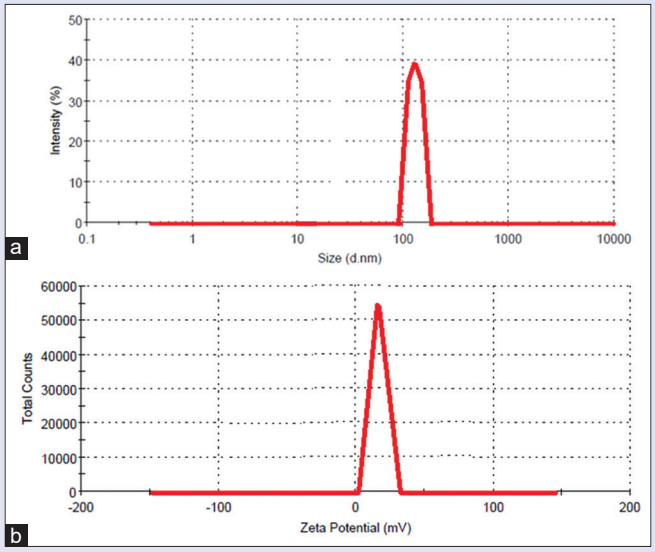

Figure 3: Globule size and size distribution (a) and zeta potential (b) of a representative formulation CLB-2

The *in vitro* release of astilbin from prepared nanoemulsions 0.1 N HCl (A) and pH 6.5 phosphate buffer saline media are shown in Figure 5. It was observed that the oil solution of astilbin (ODS) could only release approximately 11% of drug in 90 min in 0.1 N HCl. On the other hand, the nanoemulsion formulations could achieve about 4–5 fold increase in cumulative drug release in 90 min. A comparatively feeble enhancement of cumulative drug release was observed in pH 6.8 PBS release medium, in which ODS could provide approximately 40% of drug release. However, the nanoemulsion used in the study could enhance the cumulative drug release to a range of approximately 70%–80%.

The cancer chemotherapies can result in several types of liver injuries including steatosis, hepatic necrosis, liver fibrosis and sinusoidal obstruction syndrome. The cancer patients who receive OXP-treatment cycles commonly exhibit liver pathology manifestations comprising steatosis and sinusoidal injuries. In recent studies, it has been identified that oxidative stress is a very important contributing factor to various liver injuries induced by OXP therapies.[19,20] Also, it has been reported that biomarkers of oxidative stress are significantly elevated in animal models comprising mice treated with OXP cycles.[21] MDA is a product of lipid peroxidation, and its elevated levels indicate chemotherapy stress induced liver injury, which could be a result of increase in free radicals. Also, enhanced MDA levels are known to diminish other anti-oxidative factors such as SOD and GSH.

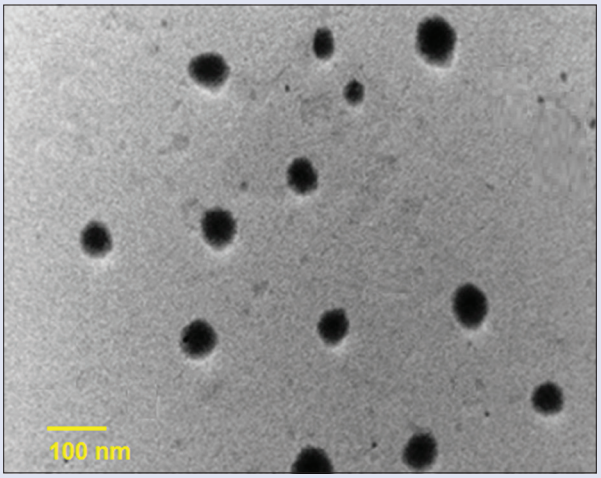

Figure 4: Transmission electron micrograph of CLB-2 (as a representative formulation)

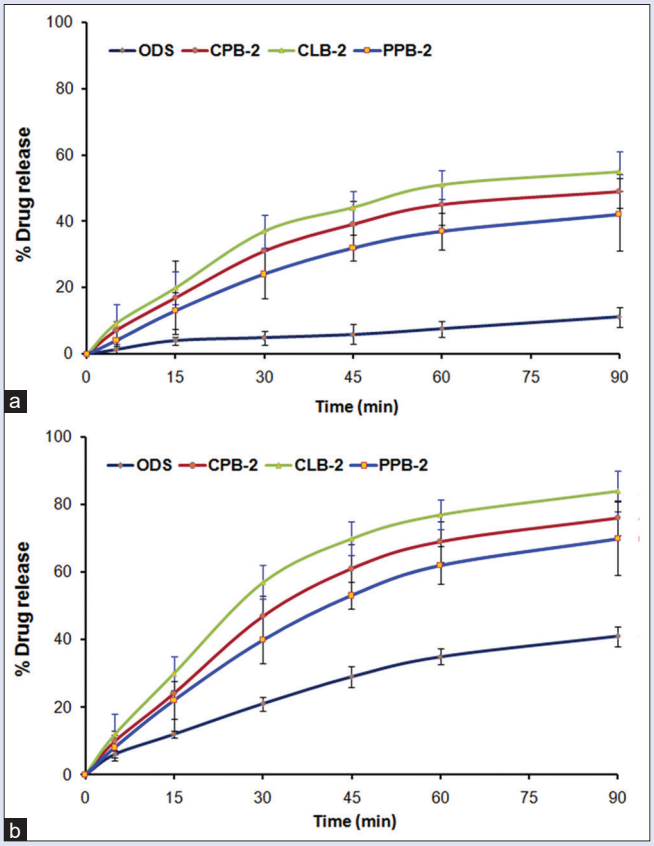

Figure 5: *In vitro* release profiles of nanoemulsions in 0.1 N HCl (a) and pH 6.5 phosphate buffer saline (b)

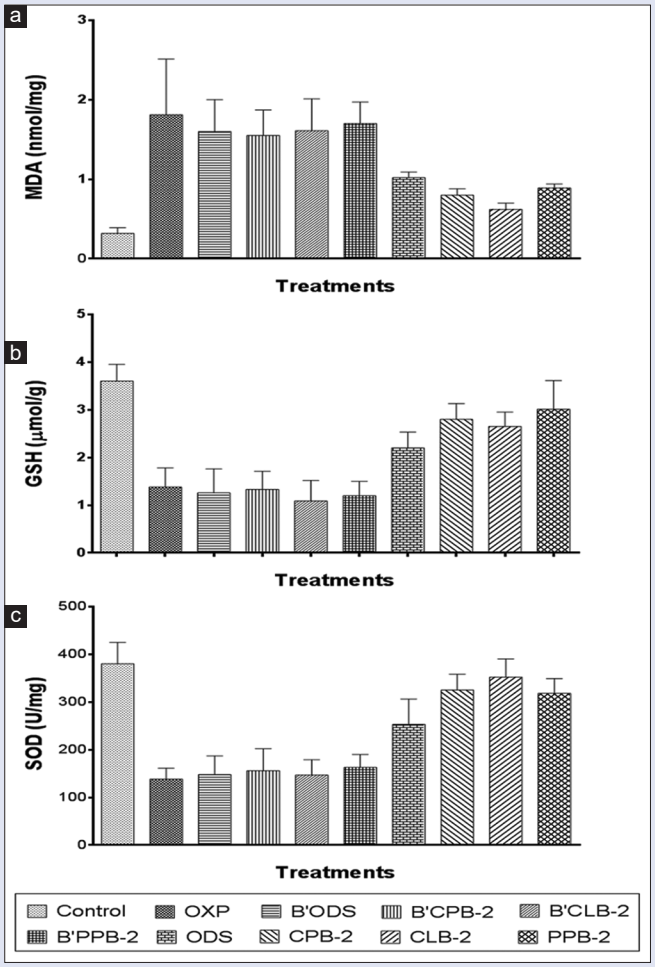

Figure 6: Results of liver oxidative stress biomarker evaluation in experimental mice. (a) MDA content b) GSH activity c) SOD activity.

These anti-oxidative factors are responsible for naturally occurring hepatoprotection in body by scavenging free radicals, which are result of stress injuries like chemotherapy. Therefore, reduced levels of these anti-oxidative molecules in body indicate higher status of liver injury, and *vice versa*. Therefore, the oxidative stress indicators in totality could play function to evaluate the status of liver pathology caused by OXP administration. Thereby, they offer exciting potential as a tool to evaluate the therapeutic potential of new medicinal products and drug combinations.

MDA is formed by degradation of polyunsaturated lipids by free radicals, and it is known to form toxic covalent protein adducts. The changes in lipid peroxidation extent in liver tissue were determined by MDA levels of various treatment groups Figure 6a. It was observed that OXP treatment significantly increased the MDA levels. Similarly, the blank formulations of selected nanoemulsions showed no effect in increased MDA levels of OXP treatment animals. There was however, a marked reduction in MDA levels of animals administered with drug solution in coconut oil (ODS). Finally, MDA levels were significantly reduced in liver tissues of animal groups treated with selected astilbin loaded nanoemulsions (CPB-2, CLB-2 and PPB-2) in comparison to that of OXP treated-and blank formulation treated animal groups.

GSH is known as a major antioxidant molecule in the body. As shown in Figure 6b, the reduced levels of GSH in liver tissue indicate stress induced liver injury. It was observed that the OXP treatment significantly reduced the GSH levels in liver tissues when compared to that of naïve animals, which indicated increased oxidative stress in the chemotherapy receiving animals. Also, the blank formulations also showed similar reduction in GSH levels. Significant improvements were observed in the liver tissues of animals treated with selected nanoemulsions. Similar to GSH, SOD is another antioxidant molecule, and liver injury causes reduction in SOD levels. As seen in Figure 6c, the animals treated

with OXP showed massive reduction in liver SOD content, indicating significant liver injury, which was also not reversed by blank treatments. The SOD levels were significantly elevated in animals administered with drug in oil solution. Also, further significant SOD level improvements were observed for animals treated with selected nanoemulsion formulations (CPB-2, CLB-2 and PPB-2) *vis-à-vis* animals treated with drug in oil solution. Therefore, the prepared nanoemulsion formulations showed excellent potential for reversing the liver injury caused by OXP treatments in experimental mice.

CONCLUSION

We successfully developed non-toxic nanoemulsion systems for astilbin, which comprised of different non-toxic food ingredients of astilbin and evaluated the potential reversing the OXP induced liver injury. We concluded that nano emulsified astilbin can be used as therapeutic agent to counter OXP associated oxidative stress.

Acknowledgements

The authors acknowledge the research support from Pharmacology Laboratory, Hospital of Chengdu University of Traditional Chinese Medicine.

Financial support and sponsorship

Nil.

Conflicts of interest

There are no conflicts of interest.

REFERENCES

1. Grothey A, Sargent D, Goldberg RM, Schmoll HJ. Survival of patients with advanced colorectal cancer improves with the availability of fluorouracil-leucovorin, irinotecan, and oxaliplatin in the course of treatment. J Clin Oncol 2004;22:1209-14.
2. Webster RG, Brain KL, Wilson RH, Grem JL, Vincent A. Oxaliplatin induces hyperexcitability at motor and autonomic neuromuscular junctions through effects on voltage-gated sodium channels. Br J Pharmacol 2005;146:1027-39.
3. Gebremedhn EG, Shortland PJ, Mahns DA. The incidence of acute oxaliplatin-induced neuropathy and its impact on treatment in the first cycle: A systematic review. BMC Cancer 2018;18:410.
4. Rubbia-Brandt L, Audard V, Sartoretti P, Roth AD, Brezault C, Le Charpentier M, *et al.* Severe hepatic sinusoidal obstruction associated with oxaliplatin-based chemotherapy in patients with metastatic colorectal cancer. Ann Oncol 2004;15:460-6.
5. Krieger PM, Tamandl D, Herberger B, Faybik P, Fleischmann E, Maresch J, *et al.* Evaluation of chemotherapy-associated liver injury in patients with colorectal cancer liver metastases using indocyanine green clearance testing. Ann Surg Oncol 2011;18:1644-50.
6. Vreuls CP, Van Den Broek MA, Winstanley A, Koek GH, Wisse E, Dejong CH, *et al.* Hepatic sinusoidal obstruction syndrome (SOS) reduces the effect of oxaliplatin in colorectal liver metastases. Histopathology 2012;61:314-8.
7. Yi HW, Lu XM, Fang F, Wang J, Xu Q. Astilbin inhibits the adhesion of T lymphocytes via decreasing TNF-alpha and its associated MMP-9 activity and CD44 expression. Int Immunopharmacol 2008;8:1467-74.
8. Xu Q, Wu F, Cao J, Chen T, Jiang J, Saiki I, *et al.* Astilbin selectively induces dysfunction of liver-infiltrating cells-novel protection from liver damage. Eur J Pharmacol 1999;377:93-100.
9. Mezghrani O, Ke X, Bourkaib N, Xu BH. Optimized self-microemulsifying drug delivery systems (SMEDDS) for enhanced oral bioavailability of astilbin. Pharmazie 2011;66:754-60.
10. Cai Y, Chen T, Xu Q. Astilbin suppresses delayed-type hypersensitivity by inhibiting lymphocyte migration. J Pharm Pharmacol 2003;55:691-6.
11. Shafiq S, Shakeel F, Talegaonkar S, Ahmad FJ, Khar RK, Ali M. Development and bioavailability assessment of ramipril nanoemulsion formulation. Eur J Pharm Biopharm 2007;66:227-43.
12. Hu L, Yang J, Liu W, Li L. Preparation and evaluation of ibuprofen-loaded microemulsion for improvement of oral bioavailability. Drug Deliv 2011;18:90-5.
13. Azevedo MI, Pereira AF, Nogueira RB, Rolim FE, Brito GA, Wong DV, *et al.* The antioxidant effects of the flavonoids rutin and quercetin inhibit oxaliplatin-induced chronic painful peripheral neuropathy. Mol Pain 2013;9:53.
14. Schwingel TE, Klein CP, Nicoletti NF, Dora CL, Hadrich G, Bica CG, *et al.* Effects of the compounds resveratrol, rutin, quercetin, and quercetin nanoemulsion on oxaliplatin-induced hepatotoxicity and neurotoxicity in mice. Naunyn Schmiedebergs Arch Pharmacol 2014;387:837-48.
15. Sethiya NK, Shah P, Rajpara A, Nagar PA, Mishra SH. Antioxidant and hepatoprotective effects of mixed micellar lipid formulation of phyllanthin and piperine in carbon tetrachloride-induced liver injury in rodents. Food Funct 2015;6:3593-603.
16. Harwansh RK, Mukherjee PK, Biswas S. Nanoemulsion as a novel carrier system for improvement of betulinic acid oral bioavailability and hepatoprotective activity. J Mol Liq 2017;237:361-71.
17. Donini C, Robinson DN, Colombo P, Giordano F, Peppas NA. Preparation of poly (methacrylic acid-g-poly (ethylene glycol)) nanospheres from methacrylic monomers for pharmaceutical applications. Int J Pharm 2002;245:83-91.
18. Pereira-Lachataignerais J, Pons R, Panizza P, Courbin L, Rouch J, López O. Study and formation of vesicle systems with low polydispersity index by ultrasound method. Chem Phys Lipids 2006;140:88-97.
19. Robinson SM, Mann J, Vasilaki A, Mathers J, Burt AD, Oakley F, *et al.* Pathogenesis of FOLFOX induced sinusoidal obstruction syndrome in a murine chemotherapy model. J Hepatol 2013;59:318-26.
20. Santoro V, Jia R, Thompson H, Nijhuis A, Jeffery R, Kiakos K, *et al.* Role of reactive oxygen species in the abrogation of oxaliplatin activity by cetuximab in colorectal cancer. J Natl Cancer Inst 2016;108:djv394.
21. Lin Y, Li Y, Hu X, Liu Z, Chen J, Lu Y, *et al.* The hepatoprotective role of reduced glutathione and its underlying mechanism in oxaliplatin-induced acute liver injury. Oncol Lett 2018;15:2266-72.